

Identification α -Amylase Inhibitors of *Vernonia amygdalina* Leaves Extract Using Metabolite Profiling Combined with Molecular Docking

Norainny Yunitasari*, Tri Joko Raharjo, Respati Tri Swasono, and Harno Dwi Pranowo

Department of Chemistry, Faculty of Mathematics and Natural Sciences, Universitas Gadjah Mada, Sekip Utara, PO BOX BLS 21, Yogyakarta 55281, Indonesia

* **Corresponding author:**

email:

yunitasari060688@mail.ugm.ac.id

Received: December 23, 2021

Accepted: February 23, 2022

DOI: 10.22146/ijc.71499

Abstract: *Vernonia amygdalina* was reported to be used as a therapy for Diabetes Mellitus (DM). One of the mechanisms of therapy DM was to inhibit the action of the α -amylase enzyme. This study aimed to prove the presence of compounds that could inhibit the action of α -amylase. *Vernonia amygdalina* leaves were macerated with methanol and partitioned into n-hexane, dichloromethane (DCM), and ethyl acetate (EtOAc). Furthermore, they were tested for α -amylase inhibitory activity and analyzed using liquid chromatography-high resolutions mass spectrometry (LC-HRMS). Molecular docking and molecular dynamics simulation (MD simulation) examined unique compounds in the extract with good activity and chromatogram results. The EtOAc extracts showed potential as α -amylase inhibitors indicated by their IC_{50} values, namely 3.0 μ g/mL. There are five unique compounds in the EtOAc extract predicted as 3-[(2Z)-3,7-dimethylocta-2,6-dien-1-yl]-2,4-dihydroxy-6-(2-phenylethyl)benzoic acid (compound 1), 2-hexylpentanedioic acid (compound 2), (2E,4E)-5-[1-hydroxy-2,6-dimethyl-4-oxo-6-({3,4,5-trihydroxy-6-(hydroxymethyl)oxan-2-yl}oxy)methyl)cyclohex-2-en-1-yl]-3-methylpenta-2,4-dienoic acid (compound 3), 3,5,5-trimethyl-4-(3-{{3,4,5-trihydroxy-6-(hydroxymethyl)oxan-1-yl}oxy}butyl)cyclohex-2-en-1-one (compound 4), and 2-[[{(6E)-2,10-dihydroxy-2,6,10-trimethyldodeca-6,11-dien-3-yl}oxy]-6-(hydroxymethyl)oxane-3,4,5-triol (compound 5). The molecular docking analysis showed that compound 3 had better interaction energy (E_i) (-8.59 kcal/mol) and inhibition constant (K_i) values (0.503 μ M) than acarbose. These data were supported by MD simulations based on the parameters of RMSD value, the radius of gyration, and protein-ligand interaction energy.

Keywords: ethyl acetate extract; diabetes mellitus; LC-HRMS; protein 4GQR; molecular dynamic simulation

■ INTRODUCTION

Indonesia is one of the countries with the highest diabetes cases, particularly type 2 diabetes mellitus (T2DM) [1]. One of the mechanisms for treating DM is to suppress the hydrolysis of glucose from carbohydrates by inhibiting the action of digestive enzymes, such as α -amylase and α -glucosidase [2]. The α -amylase is the first digestive enzyme that breaks down dietary carbohydrates such as starch into simpler parts in the digestive system, which would then be degraded further by the α -glucosidase into glucose which is readily absorbed and enters the bloodstream [3]. Inhibition of the α -amylase is

an important molecular target for the treatment of type 2 DM [4]. Acarbose is one of the DM medicines that act as an α -glucosidase inhibitor [5]. A combination of α -amylase and α -glucosidase could be a potential approach to treat DM. However, none of the DM medicine has been reported to inhibit α -amylase.

Vernonia amygdalina leaves or often known as insulin leaves, are believed to be diabetes mellitus drugs. *Vernonia amygdalina* plant, commonly known as African leaves, is consumed by people with diabetes for therapeutic purposes in African countries [6]. The use of *Vernonia amygdalina* leaves for the treatment of DM is also carried out by people in Central Indonesia

(Makassar). Drinking tea from *Vernonia amygdalina* has been reported to be successful in lowering blood glucose levels [7]. This plant is also reported to treat various diseases other than DM [8]. These biological effects could be attributed to polyphenols in the extract, especially dicaffeoyl-quinic acid and its isomers [9]. In other studies, *Vernonia amygdalina* leaves were also shown to have the potential as a natural source for managing diabetes. In vitro, the extract of this plant was proven to contain a lot of mineral elements (potassium, magnesium, and calcium) and a little content of chromium through the microwave-assisted extraction method [10].

Phytochemicals in plants are very complex, with various concentrations. High-resolution MS was reported can be employed to do a high throughput metabolite profile. LC-HRMS was reported to identify compounds in large quantities in a short time. LC-HRMS was a high-resolution mass spectrometry linked to a database of compounds. Previous research identified 120 compounds from *Diaphragma juglandis*, of which 20 compounds are bioactive compounds, using LC-HRMS [11]. From the results of the analysis with LC-HRMS, it could be seen the structure of the identified compounds. This information helped perform in silico tests. An in-silico approach, namely through molecular docking, could be used to see if a compound had the potential to act as an α -amylase inhibitor [8-7,11]. In silico research had been conducted to prove to inhibit the work of α -amylase and α -glucosidase by several compounds. Several compounds were able to inhibit the work of α -amylase in silico, including Luteolin (LUT), Hesperetin (HES), and Quercetin (QUE) [12]. The compounds that could inhibit the action of α -glucosidase in silico were myricetin-3-O-rhamnoside (myricitrin) and epigallocatechin-3-gallate (EGCG) [1]. Molecular docking could be a valuable tool for proving an activity [13] and facilitating the discovery of new compounds in inhibiting α -amylase [14].

This study aimed to identify the secondary metabolites of *Vernonia amygdalina* that could be responsible for the antidiabetic activity, especially as an α -amylase inhibitor. Metabolite profile of the active extract followed by docking the discovered compounds from the

profile used as tools to accomplish the goal.

■ EXPERIMENTAL SECTION

Materials

Fresh leaves of *Vernonia amygdalina* were obtained from a self-grown plant. The authenticity of the plant was confirmed by The Plants Systematics Laboratory, Faculty of Biology, Universitas Gadjah Mada. All chemicals used were the analytical reagent grade, such as methanol (MeOH), n-hexane, dichloromethane (DCM), and ethyl acetate (EtOAc), and were commercially purchased from Merck (Darmstadt, Germany). α -amylase from hog pancreas was purchased from Sigma USA. Dimethyl sulfoxide (DMSO) and 3,5-dinitrosalicylic acid (DNSA) were purchased from Sigma-Aldrich.

Instrumentation

The instruments used were rotary evaporator (Buchi), incubator oven (Mettler), LC-HRMS Thermo Exactive Orbitrap (Thermo Scientific), and spectrophotometer UV-vis (Thermo Fisher Scientific G10S). Molecular docking assay was implemented using AutoDock Tools (ADT, version: 1.5.7), provided with the AutoDock 4.2 package (Autodock 4.2, Autogrid 4.2, AD4.1_bound, and AD4_parameters). Docking and MD simulation were running in a PC Computer using an AMD ThreadRipper 3970X processor.

Procedure

Plant extract preparation

Fresh leaves were dried in the shade with the sunlight exposure and aerated for 3-4 days. The dried leaves were powdered using a blender machine (Philips). Powdered leaves (500 g) of *Vernonia amygdalina* were macerated with 2000 mL methanol (MeOH) at room temperature for 3×24 h for each extraction. The MeOH extracts were concentrated by a rotary evaporator at 40 °C to 100 mL. The concentrated methanol extracts were partitioned with hexane-water (1:1) followed by n-hexane, DCM-water (3:1), and DCM. All extracts of partition were evaporated under vacuum at 40 °C. All extracts were stored in the refrigerator until further use.

In vitro α -amylase inhibitory studies

The method used for the α -amylase inhibition assay was the 3,5-dinitrosalicylic acid (DNSA) method [13-14]. Each extract was dissolved in a minimum amount of 10% DMSO and was further dissolved in buffer ((Na₂HPO₄/NaH₂PO₄ (0.02 M), NaCl (0.006 M) at pH 6.9). The 200 μ L of α -amylase solution (5 units/mL) was mixed with 200 μ L of the extract in a test tube and was incubated at 30 °C for 10 min. The test tubes were added 200 μ L of the starch solution (1% in water (w/v)) and incubated for 3 min. The reaction was terminated by adding 200 μ L DNSA reagent (12 g of sodium potassium tartrate tetrahydrate in 8.0 mL of 2 M NaOH and 20 mL of 96 mM of 3,5-dinitrosalicylic acid solution) and boiled at 85–90 °C for 10 min. The mixture was cooled to ambient temperature and was diluted with 5 mL of distilled water, and the absorbance was measured at 540 nm using a UV-Visible spectrophotometer. The blank with 100% enzyme activity was prepared by replacing the plant extract with 200 μ L of the buffer. A blank sample was prepared using the plant extract at each concentration in the absence of the enzyme solution, while acarbose (100 μ g/mL–2 μ g/mL) was used as a positive control. The α -amylase inhibitory activity was expressed as percent inhibition and was calculated using the equation given below: The % α -amylase inhibition was plotted against the extract concentration, and the IC₅₀ values were obtained from the graph.

$$\% \alpha \text{ amylase inhibition} = 100 \times \frac{\text{Abs}_{100\% \text{ Control}} - \text{Abs}_{\text{Sample}}}{\text{Abs}_{100\% \text{ Control}}}$$

Using LC-HRMS analysis

The methanol extract, *n*-hexane extract, DCM extract, and EtOAc extract were analyzed using LC-HRMS. Five mg of extract dissolved in 5 mL of methanol then filtered with 0.2 μ m PTFE membrane and 5 μ L sample was injected. The LC-HRMS employed UHPLC Vanquish Tandem Q Exactive Plus Orbitrap LC-HRMS ThermoScientific. The column used was Accucore C18, 100 \times 2.1 mm, 1.5 μ m (ThermoScientific). The eluents used were H₂O with 0.1% formic acid (A) and acetonitrile with 0.1% formic acid (B). The flow rate was 0.2 mL/min. used gradient 5–60% B (0–15 min), flowed by 60–95% B (15–22 min), and kept until 25 min before finally

returning to 5%B (25–30 min). The MS/MS scan was set at *m/z* = 200–2000 with full scan and ddMS2 using positive and negative mode. The raw data was then analyzed using compound discoverer 2.0 software using untargeted metabolomics. The precursor ions and their fragmentation pattern of particular peaks on the sample chromatogram were matched with the mzCloud compound database during the identification process. The results of LC-HRMS were clarified by comparing the measured molecular weight with the proposed molecular weight. After that, check the molecular formula at www.chemcals.com and the structural formula at www.pubchem.com.

Molecular docking studies

Ligand preparation. The ligand structure of compounds 1 to 5 was obtained from the results of the LC-HRMS analysis. These structures were drawn using Marvin [15] in 2D format, and the clean 3D structure was optimized using the Orca program [16]. A Density functional theory (DFT) based on the proposed three-fold corrected (3c) Hartree-Fock method, termed PBEh-3c, was applied to optimize geometry ligand structure [17]. The optimized structure of the ligand was loaded partial charge by Gasteiger charge and kept in *.pdbqt format using AutodockTools 1.5.7.

Receptor preparation. The protein structure was downloaded from the protein data bank with PDB ID 4GQR. For docking purposes, water molecules were clean, and the Co-Crystal ligand code in Myricetin (MYC) was separate. Hydrogen atoms were added to the protein structure using the PyMOL program. Partial charges using the Gasteiger charge were loaded into the structure by AutodockTools 1.5.7. The Final file *.pdbqt was ready for docking.

Grid and docking parameter File. Using MYC ligand reference, the grid box for the search location was centered at [13.047 14.631 39.633] coordinate. The grid box dimensions were 60 \times 60 \times 60 Å with a 0.375 Å spacing. Autodock 4.2.6 was used as a docking program. Lamarckian Genetic Algorithm was used as a search parameter with *ga_run* was 100 times running, *ga_pop_size* was set to 300 and *ga_num_evals* using comprehensive evaluation, 25000000. Docking results

are visualized using Ligplot software version 4.4.2 (EMBL-EBI, Cambridgeshire, UK).

Molecular dynamics (MD) simulation

MD preparation. Complex structure from the best results of the docking step was used as the initial structure for MD simulation. Preparation uses the pdb4amber module for checking gaps, adding hydrogen, and missing atoms and residues. The protonation state (pK) of amino acid was computed using H++ Web Service (<http://newbiophysics.cs.vt.edu/H++/>). Ligands were parameterized using semi-empirical AM1-BCC methods using the Antechamber program. The complex protein-ligand was solvated using the TIP3P water model in a 14 Å cubic box. The final topology file (*.top) and coordinate file (*.crd) were built using the LEap module from AMBER20.

MD step. Molecular dynamics simulation consists of four steps. They are minimization of energy, heating, equilibration, and production. Energy minimization is needed to eliminate steric hindrance and bad contact. Energy minimization consists of 5 stages. Each stage has a different constraint value that gradually decreases. The last stage of minimization was set to be free from constraint. The combined algorithm, Steepest Descent, and Conjugate Gradient were used in the minimization step. The heating step is needed to make the solvent reach the final temperature, 300 K. The simulation system was set to the NVT ensemble when entering the heating step, and a small constraint of about 10 kcal/mol was applied only for C-alpha atoms. The Langevin method was used with γ_{ln} 1 for the heating process. The Equilibration step was to get the appropriate density of the system. In this step, an NPT ensemble was used, and a constraint from the heating process was released gradually. The final step, production run, was the molecular dynamics without any constraint and in natural conditions. The NPT ensemble was used from the equilibration step. The Periodic Boundary Condition was set to on, 9 Å was used as a cutoff, and 2 fs was used as timestep. Production of data evaluations was divided into 50 parts. Each part equals 2 ns simulation time and gives 100 ns in total. All MD step was carried out using the pmemd module as part of the AMBER program [18].

RESULTS AND DISCUSSION

α -Amylase Inhibition Activity

The inhibitory ability of the extract was observed from their IC_{50} value. The smaller IC_{50} value indicated a higher ability to inhibit α -amylase. Acarbose, a widely used and marketed antidiabetic drug, was used as a positive control. Acarbose worked by inhibiting α -glycosidase and was chosen as a positive control because no commercial anti-DM worked by inhibiting α -amylase [14]. Acarbose as a positive control in α -amylase inhibition was not as good as a positive control in α -glucosidase inhibition. In the study on *Vitex doniana* leaf extract, the IC_{50} value of α -glucosidase inhibition was smaller than when inhibited α -amylase, namely 55.59 μ g/mL and 256.66 μ g/mL, respectively [19].

The results of the α -amylase inhibition assay of the four types of extracts are shown in Table 1. The EtOAc extract was the extract that had the smallest IC_{50} value, namely 3.0 μ g/mL. This extract had a smaller IC_{50} value than the positive control. These findings indicated that the EtOAc from *Vernonia amygdalina* was potent to be further studied in searching for the compounds for the α -amylase inhibitor. In another study, EtOAc extract from *Eugenia dysenterica* leaves exhibited inhibitory capability against α -amylase, with an inhibitory ability of above 50% at 10 μ g/mL [20]. Similar results were also found in the study on *Vitex doniana* leaf extract, where the EtOAc extract had the smallest IC_{50} value [19]. The IC_{50} value of α -amylase inhibition from the *Vernonia amygdalina* leaf extract was not as strong as the α -amylase inhibition from the *Vitex doniana* leaf extract, the IC_{50} values were 3.0 μ g/mL and 1.67 μ g/mL, respectively.

Table 1. The results of α -amylase inhibition assay on various extracts of *Vernonia amygdalina* and acarbose

No.	Extract	IC_{50} (μ g/mL)
1	Methanol	5.0
2	<i>n</i> -hexane	29.3
3	DCM	6.7
4	EtOAc	3.0
5	Acarbose	23.6

Profiling of Compounds Using LC-HRMS Analysis

LC-HRMS results showed that 7 compounds only appeared in the EtOAc extract. There were 5 of them had good chromatogram results; namely, a single signal only appeared in the sample (Table 2). These compounds had not been reported as inhibitors of α -amylase.

The peak at RT 10.005 min identified the presence of compound 1 and was characterized by fragment ions at m/z 99.87447 and 136.13499. At the RT 11.347 min, compound 2 was identified and indicated by the fragment

ions at m/z 57.03340, 61.98717, and 85.51666. Compound 3 was identified at RT 7.722 min and characterized by the fragment ions at m/z 135.08040 and 83.02869. Fragment ions at m/z 101.02333, 137.02327, and 161.02336 indicated the presence of compound 4 and exited at RT 8.290 min. Compound 5 was characterized by the presence of fragment ions at m/z 68.86910, 145.20244, and 163.03885 and exited at RT 8.739 min. One of the LC-HRMS results could be seen in Fig. 1.

Table 2. LC-HRMS data of unique compounds in the EtOAc extract

RT (min)	Compounds		Formula	Molecular weight (MW)	Production (m/z)
	No.	Name			
10.005	Compound 1	3-[(2Z)-3,7-dimethylocta-2,6-dien-1-yl]-2,4-dihydroxy-6-(2-phenylethyl)benzoid acid	C ₂₅ H ₃₀ O ₄	394.21441	99.87447; 136.13499
11.347	Compound 2	2-hexylpentanedioic acid	C ₁₁ H ₂₀ O ₄	216.13616	57.03340; 61.98717; 85.51666
7.722	Compound 3	(2E,4E)-5-[1-hydroxy-2,6-dimethyl-4-oxo-6-({3,4,5-trihydroxy-6-(hydroxymethyl) oxan-2-yl] oxy} methyl) cyclohex-2-en-1-yl]-3-methylpenta-2,4-dienoic acid	C ₂₁ H ₃₀ O ₁₀	442.1839	135.08040; 83.02869
8.290	Compound 4	3,5,5-trimethyl-4-(3-{{3,4,5-trihydroxy-6-(hydroxymethyl) oxan-1yl} oxy} butyl) cyclohex-2-en-1-one	C ₁₉ H ₃₂ O ₇	372.214805	101.02333; 137.02327; 161.02336
8.739	Compound 5	2-{{(6E)-2,10-dihydroxy-2,6,10-trimethyldodeca-6,11-dien-3-yl} oxy}-6-(hydroxymethyl) oxane-3,4,5-triol	C ₂₁ H ₃₈ O ₈	418.25667	68.86910; 145.20244; 163.03885

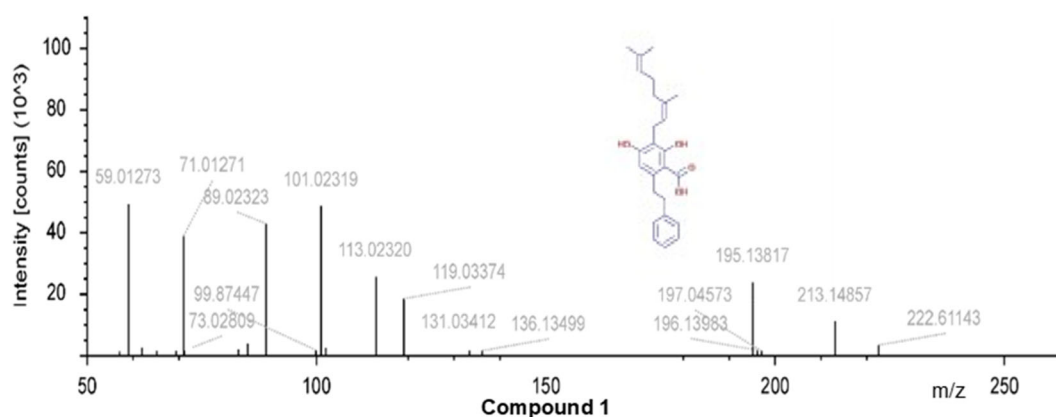


Fig 1. The LC-HRMS results in EtOAc extract

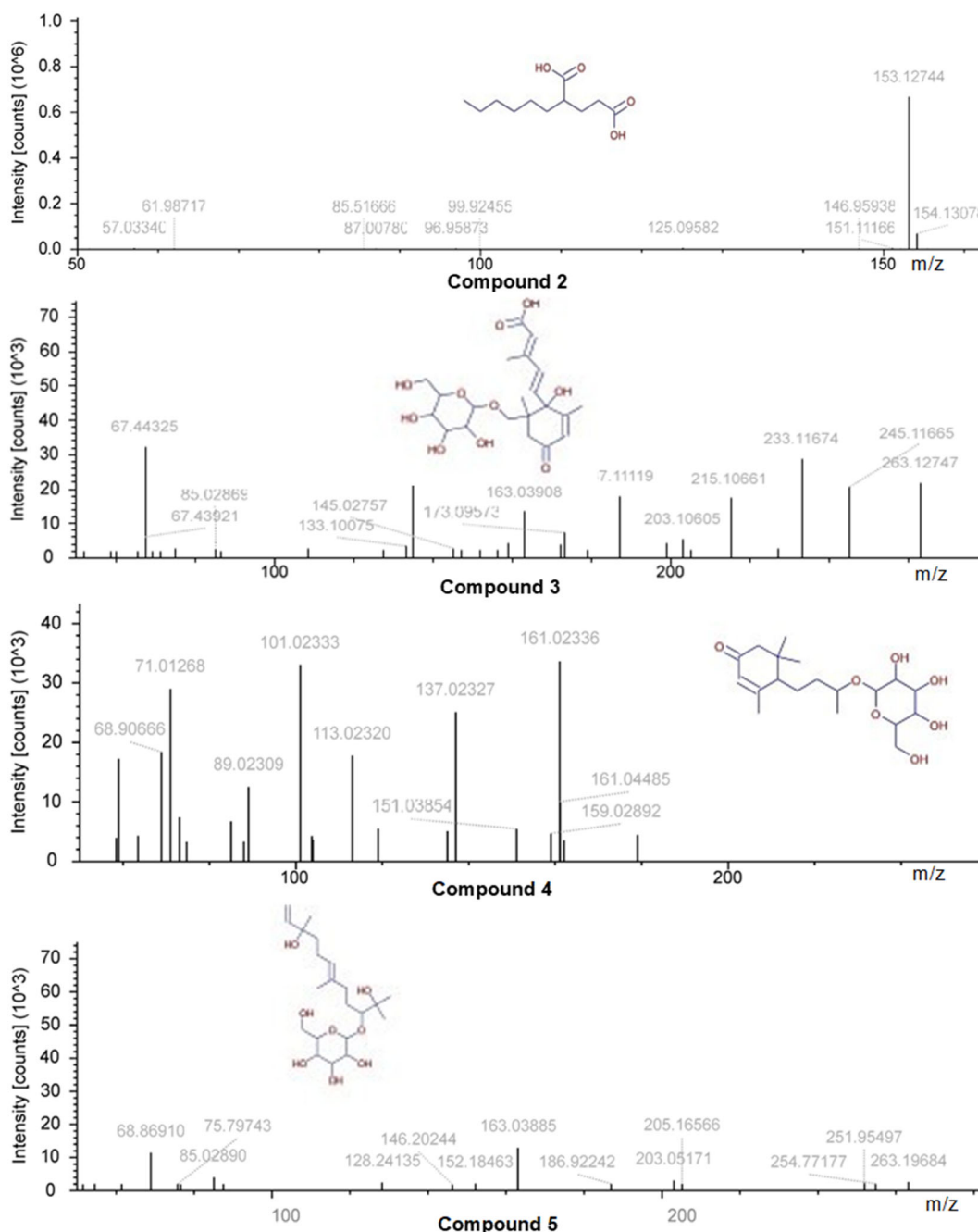


Fig 1. The LC-HRMS results in EtOAc extract (Continued)

Molecular Docking Assay

Re-docking results

The RMSD value obtained from the re-docking results was 1.998 Å. This value was obtained from the second conformation, and the interaction energy (E_i) was -7.16 kcal/mol. Re-docking MYC ligand was used as a validating docking parameter since MYC are Co-Crystal ligands of 4GQR (Fig. 2).

The type of interaction between MYC and human pancreatic alpha-amylase before and after re-docking was shown in Fig. 3. Hydrogen bond interactions between MYC and amino acid residues Asp197, Gln63, and Trp59 could still be seen. On the results of re-docking could also be obtained the value of the inhibition constant that was 5.6 μ M.

Docking results

The docking results of 5 unique compounds in the EtOAc extract can be seen in Fig. 4. These results indicated that not all the docked compounds occupied the active site of the human pancreas α -amylase (Table 3). Human pancreas α -amylase had an active site on Asp197, Glu233, and Asp300 [21]. At the same time, acarbose (as a positive control and as a diabetes drug) inhibited the action of α -amylase through its active site, which was attached to amino acid residues Asp197, Glu233, and Asp300 (Fig. 5).

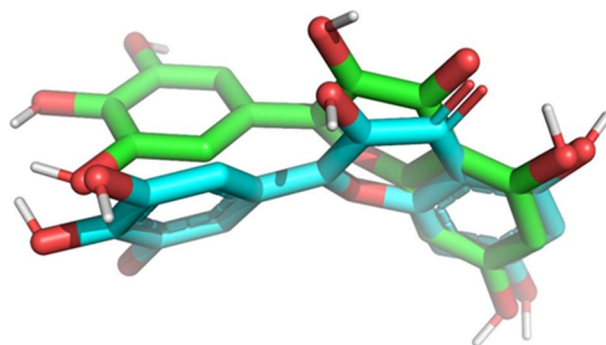


Fig 2. Re-docking MYC ligand

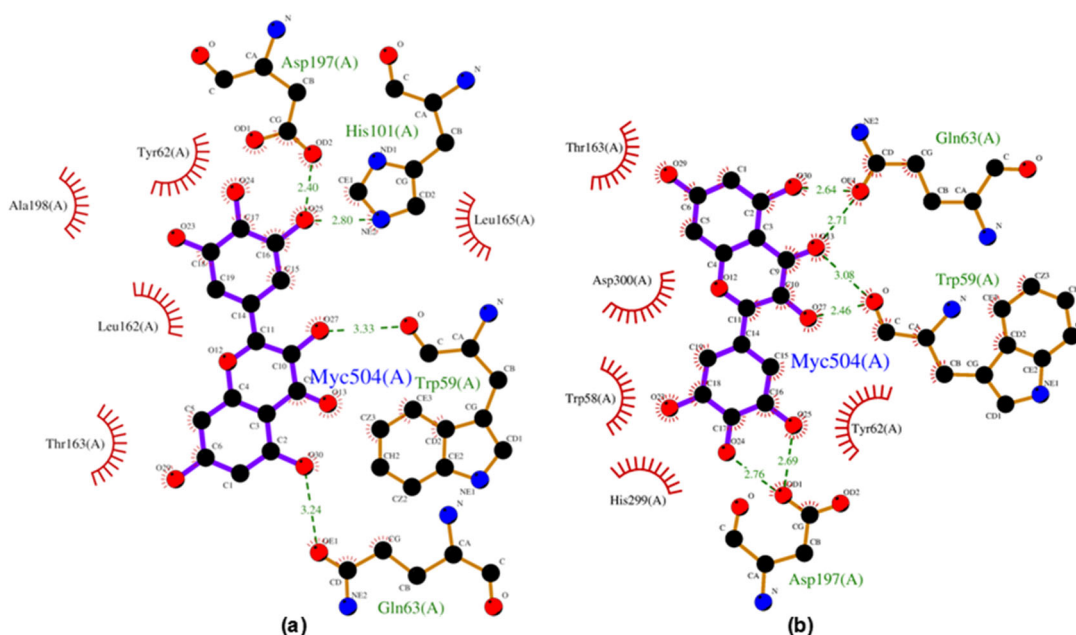


Fig 3. (a) Complex between 4GQR and MYC co-crystals, and (b) Complex between 4GQR and MYC (re-docking)

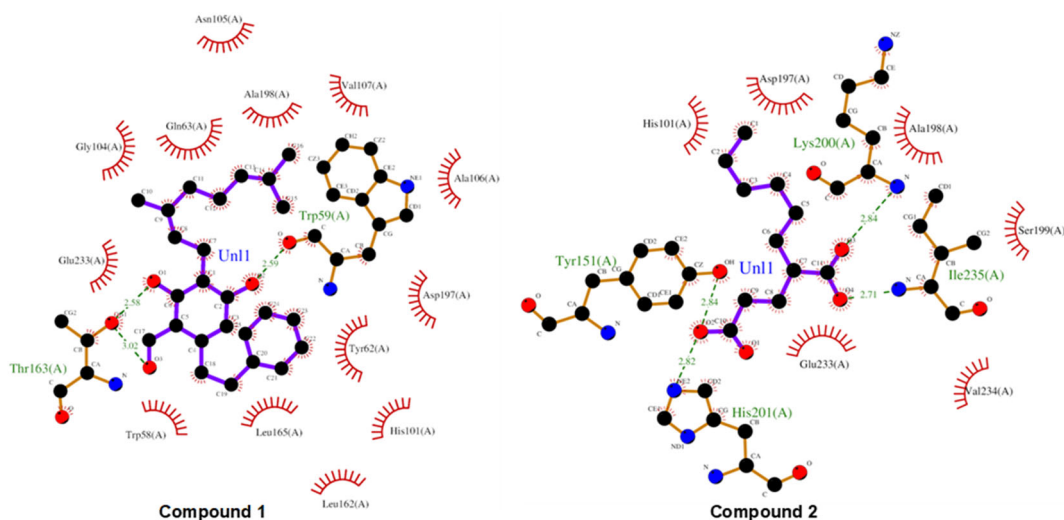


Fig 4. Docking of the unique compounds in the EtOAc extract

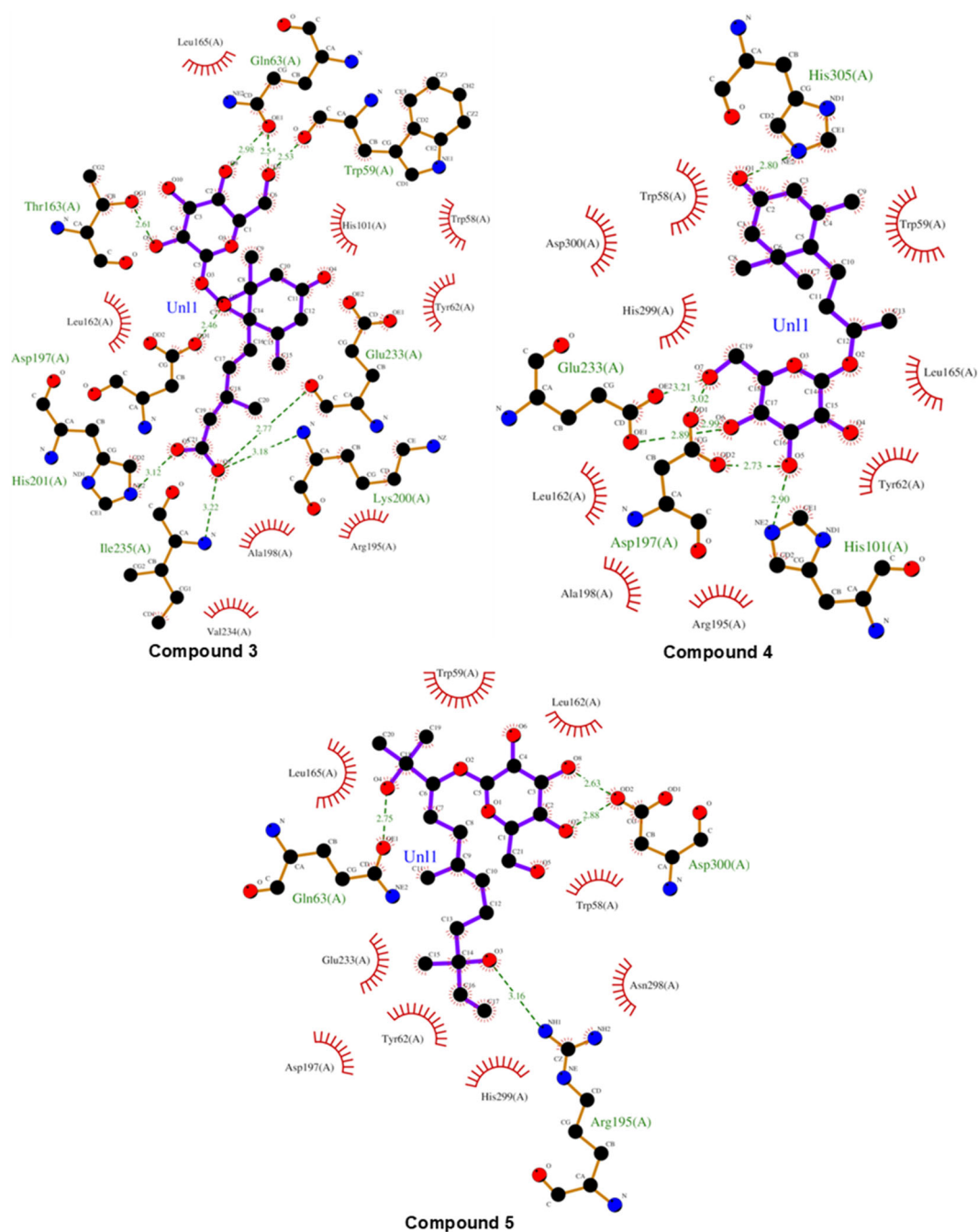


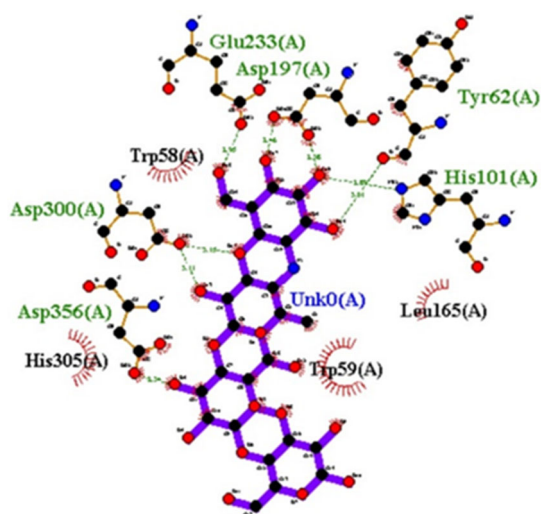
Fig 4. Docking of the unique compounds in the EtOAc extract (Continued)

Based on E_i and K_i values, there were two of five unique compounds in the EtOAc extract, which had a better value than the E_i and K_i values of the original ligand and acarbose, namely compound 3 and compound 4 (Table 4). A drug candidate could be better than the standard drug if E_i and K_i were lower than the standard drug [22]. The more negative the interaction energy, the

more stable the ligand interaction with the protein. A negative value of the interaction energy indicated that the binding of the ligand to the protein was a spontaneous process [23]. The value of the inhibition constant could be said to be proportional to the IC_{50} value with the assumptions: 1) for competitive inhibition, the substrate concentration is close to zero;

Table 3. The hydrogen bond distance of each compound in the molecular docking analysis

	Acarbose	Compound 1	Compound 2	Compound 3	Compound 4	Compound 5	
Distance to amino acid residues (Å)	Asp197	2.38; 2.46	-	-	3.12	3.02	-
	Asp300	3.11; 3.15	-	-	-	-	2.63; 2.88
	Glu233	2.95	-	-	2.77	2.89; 3.21	-
	Asp356	2.34	-	-	-	-	-
	Tyr62	3.01	-	-	-	-	-
	His101	2.89	-	-	-	2.90	-
	Thr163	-	2.58; 3.02	-	2.61	-	-
	Lys200	-	-	2.84	3.18	-	-
	Ile235	-	-	2.71	3.22	-	-
	Gln63	-	-	-	2.54; 2.98	-	2.75
	Trp59	-	2.59	-	2.53	-	-
	Tyr151	-	-	2.82	-	-	-
	His201	-	-	2.82	3.12	-	-
	His305	-	-	-	-	2.80	-
	Arg195	-	-	-	-	-	3.16

**Fig 5.** Results of docking acarbose with alpha-amylase (PDB ID 4GQR)**Table 4.** List of interaction energy values and inhibition constants

Name	Interaction energy/ E_i (kcal/mol)	Inhibition constants/ K_i (μM)
Acarbose	-6.44	19.09
Compound 1	-6.15	31.14
Compound 2	-4.34	659.75
Compound 3	-8.59	0.503
Compound 4	-7.26	4.75
Compound 5	-5.70	66.76

and 2) for non-competitive inhibition, the substrate concentration is infinite. For K_i , smaller values denote tighter binding [24].

The location of the hydrogen bond formed between compound 3 and α -amylase was on the active site of α -amylase, namely on the amino acid residues Asp197 and Glu233 and in the amino acid residues Thr163, Lys200, Ile235, Gln63, Trp59, and His201. Compound 4 inhibited the protein's active site, notably the Asp197 and Glu233 amino acid residues, and established hydrogen bonds with the His101 and His305 amino acid residues. The number of hydrogen bonds formed between compounds 3 and 4 with α -amylase was what causes compounds 3 and 4 to have the most negligible interaction energy and inhibition constant compared to other ligands.

The value of the interaction energy and the inhibition constant of compounds 1, 2, and 5 was less good than acarbose. These facts were possible due to the absence of hydrogen bonds formed with the active site of α -amylase.

Molecular Dynamics Simulation Analysis

This MD simulation analysis was helpful in the analysis of molecular docking results [25]. There were

several parameters in the MD simulation, including Root Mean Square Deviation (RMSD), Radius of Gyration, Root Mean Square Fluctuation (RMSF), and Protein-Ligand Interaction Energy.

Root mean square deviation (RMSD)

RMSD was a measure of conformational change concerning the reference conformation. In this simulation, the reference used was the initial confirmation at the start of the production run stage. The conformational changes of the five ligands are shown in Fig. 6. Compound 5 had a high fluctuation at 10 ns. There were also high fluctuations in compound 2 when after 40 ns. However,

compound 3 has relatively no high fluctuations. At 20 ns to 40 ns, the five compounds converged in 1.25 to 1.5 Å. Overall the RMSD of all compounds/ligands was stable in the change range of 1.5 Å. This RMSD result showed that the presence of the bound ligand did not significantly change the conformation of the protein, so it did not change the protein's function.

Radius of gyration

The radius of gyration showed the compactness of the structure and could see whether the structure was swelling or shrinking. The value of the radius of gyration of the five compounds can be seen in Fig. 7. The radius

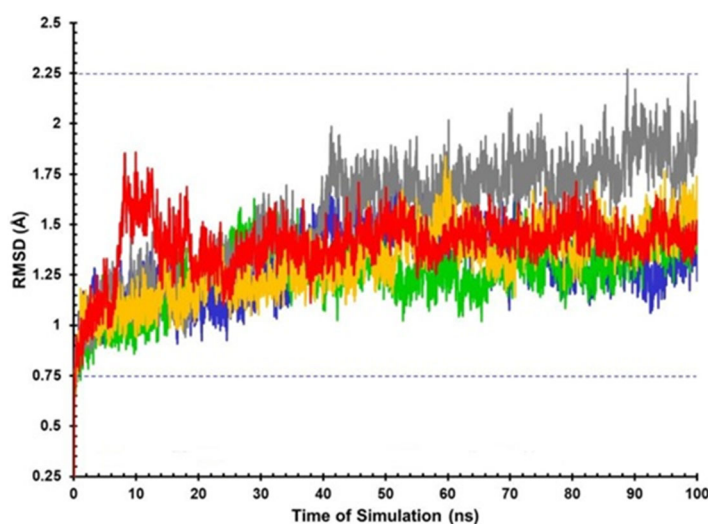


Fig 6. The conformational change of the five compounds during simulation time 100ns (blue: compound 1; grey: compound 2; green: compound 3; yellow: compound 4; and red: compound 5)

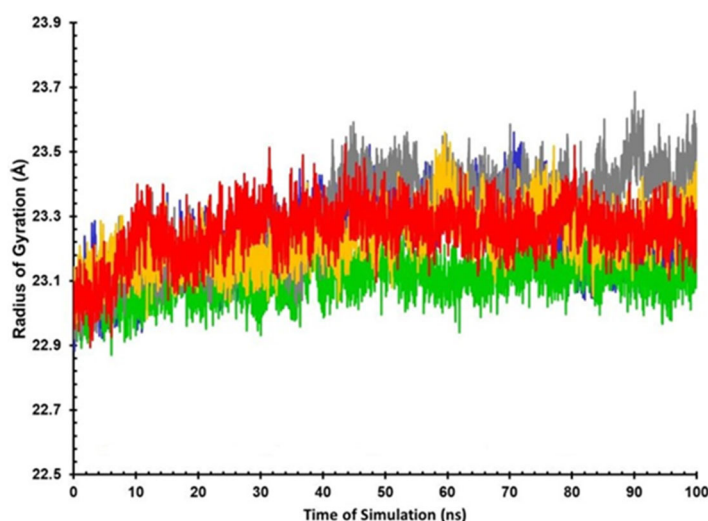


Fig 7. The radius of gyration of the five compounds during simulation time 100 ns (blue: compound 1; grey: compound 2; green: compound 3; yellow: compound 4; and red: compound 5)

of gyration showed the globular shape of the protein structure. The graph showed the shape of the globular structure was not swelling. The value of the radius of gyration had a slight difference in the conformational system of compound 3. The results of the radius of gyration analysis were in line with the results of the RMSD analysis, which showed that compound 3 did not have high fluctuations.

Root mean square fluctuation (RMSF)

RMSF was the dynamic fluctuation of each amino acid residue in the protein structure. This fluctuation

indicated a particular part of a protein structure that could have certain flexibility. Fluctuations that were not high allow for relatively easy interactions with ligands (Fig. 8). The RMSF graph showed the portion of amino acid residues that could have hydrogen bond interaction and other interactions, including Asp197, Glu233, Ala198, Leu162, His101, Trp59, and Tyr62. Furthermore, these residues could be considered when designing drugs targeting α -amylase. According to the docking results, compound 3 could form a hydrogen bond with amino acid residues Asp197, Glu233, and Trp59. Compound 4

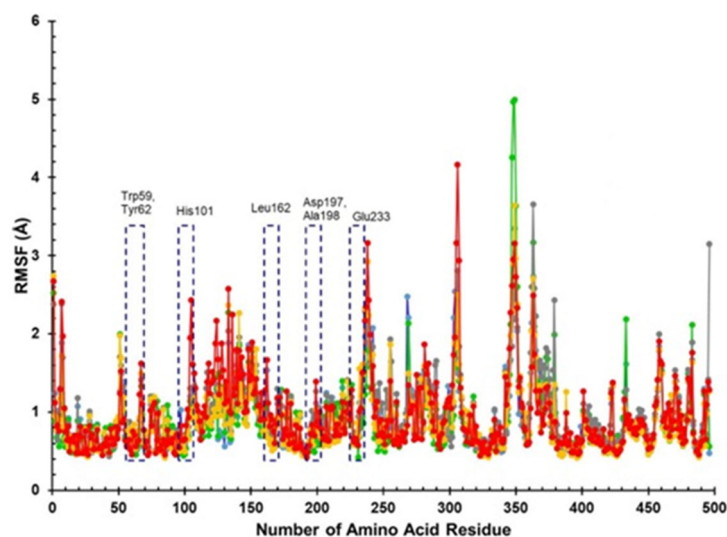


Fig 8. RMSF data (blue: compound 1; grey: compound 2; green: compound 3; yellow: compound 4; and red: compound 5)

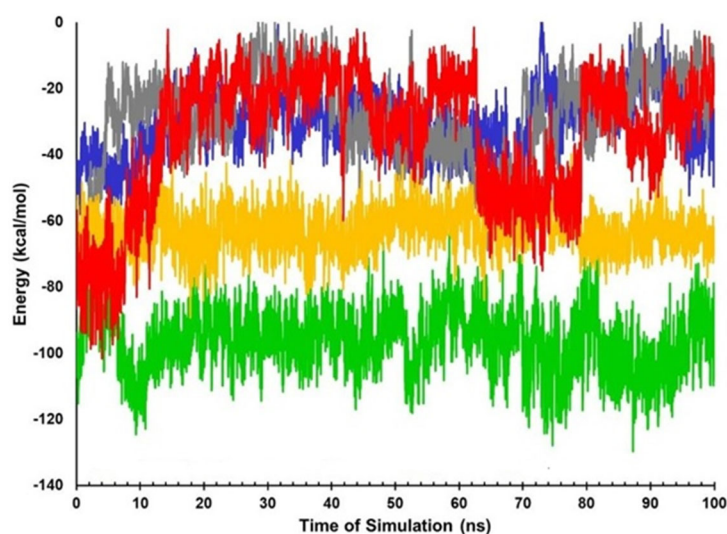


Fig 9. Protein-ligand interaction energy (blue: compound 1; grey: compound 2; green: compound 3; yellow: compound 4; and red: compound 5)

could form hydrogen bonds with amino acid residues Asp197, Glu233, and His101.

Protein-ligand interaction energy

The interaction energy was calculated using NamdEnergy from the NAMD program by looking at the non-bond interaction between protein and ligands. The calculated interactions included Van der Waals and electrostatic interactions. The total energy was the sum of the two energies—the more negative, the stronger the interaction between the ligand and the receptor (Fig. 9). Compounds 3 and 4 had the most substantial interaction energy values, with an average of -96.45 and -62.92 kcal/mol, respectively. Based on the graph, the interaction of the two ligands was relatively stable, only slightly experiencing insignificant fluctuations. The other three ligands appeared to be binding unstable.

CONCLUSION

The extract with the most potential as an α -amylase inhibitor was the EtOAc extract. From the LC-HRMS analysis, the EtOAc extract contained seven unique compounds. Five of the seven unique compounds had good chromatograms and were analyzed by molecular docking and MD simulations. This analysis could prove compounds with potential as α -amylase inhibitors, including compound 3.

ACKNOWLEDGMENTS

This work was supported by Lembaga Pengelola Dana Pendidikan (LPDP). This study is part of dissertation research.

AUTHOR CONTRIBUTIONS

The first author worked in the laboratory. The second author was the supervisor of the LC-HRMS analysis. The third author was the supervisor of the extraction process. The fourth author was the supervisor in the docking analysis and MD simulation.

REFERENCES

- [1] Syabana, M.A., Yuliana, N.D., Batubara, I., and Fardiaz, D., 2022, α -Glucosidase inhibitors from *Syzygium polyanthum* (Wight) Walp leaves as revealed by metabolomics and in silico approaches, *J. Ethnopharmacol.*, 282, 114618.
- [2] Liu, S., Yu, Z., Zhu, H., Zhang, W., and Chen, Y., 2016, *In vitro* α -glucosidase inhibitory activity of isolated fractions from water extract of Qingzhuan dark tea, *BMC Complementary Altern. Med.*, 16 (1), 378.
- [3] Alqahtani, A.S., Hidayathulla, S., Rehman, M.T., ElGamal, A.A., Al-Massarani, S., Razmovski-Naumovski, V., Alqahtani, M.S., El Dib, R.A., and AlAjmi, M.F., 2020, Alpha-amylase and alpha-glucosidase enzyme inhibition and antioxidant potential of 3-oxolupenal and katononic acid isolated from *Nuxia oppositifolia*, *Biomolecules*, 10 (1), 61.
- [4] Ganesan, M.S., Raja, K.K., Narasimhan, K., Murugesan, S., and Kumar, B.K., 2020, Design, synthesis, α -amylase inhibition and *in silico* docking study of novel quinoline bearing proline derivatives, *J. Mol. Struct.*, 1208, 127873.
- [5] Wyne, K., and Bakris, G.L., 2007, "Control of Blood Glucose and Insulin Resistance" in *Comprehensive Hypertension*, Eds. Lip, G.Y.H., and Hall, J.E., Mosby, Philadelphia, US, 1105–1112.
- [6] Ndip, R.N., Tanih, N.F., and Kuete, V., 2013, "Antidiabetes Activity of African Medicinal Plants" in *Medicinal Plant Research in Africa*, Eds. Kuete, V., Elsevier, Oxford, 753–786.
- [7] Halim, A.M., Sirajuddin, S., Bahar, B., Jafar, N., Syam, A., and Masni, 2020, The effect of African leaf herbal tea on fast blood glucose on centration of prediabetes teachers in Makassar city, *Enferm. Clin.*, 30, 261–264.
- [8] Egharevba, G.O., Dosumu, O.O., Oguntoye, S.O., Njinga, N.S., Dahunsi, S.O., Hamid, A.A., Anand, A., Amtul, Z., and Priyanka, U., 2019, Antidiabetic, antioxidant and antimicrobial activities of extracts of *Tephrosia bracteolata* leaves, *Heliyon*, 5 (8), e02275.
- [9] Ong, K.W., Hsu, A., Song, L., Huang, D., and Tan, B.K.H., 2011, Polyphenols-rich *Vernonia amygdalina* shows antidiabetic effects in streptozotocin-induced diabetic rats, *J. Ethnopharmacol.*, 133 (2), 598–607.

- [10] Alara, O.R., and Abdurahman, N.H., 2019, Antidiabetic activity and mineral elements evaluation of *Vernonia amygdalina* leaves obtained from Malaysia, *J. Res. Pharm.*, 23 (3), 514–521.
- [11] Martinez-Gonzalez, A.I., Díaz-Sánchez, Á.G., de la Rosa, L.A., Bustos-Jaimes, I., and Alvarez-Parrilla, E., 2019, Inhibition of α -amylase by flavonoids: Structure activity relationship (SAR), *Spectrochim. Acta, Part A*, 206, 437–447.
- [12] Miller, G.L., 1959, Use of dinitrosalicylic acid reagent for determination of reducing sugar, *Anal. Chem.*, 31 (3), 426–428.
- [13] Wickramaratne, M.N., Punchihewa, J.C., and Wickramaratne, D.B.M., 2016, *In-vitro* alpha amylase inhibitory activity of the leaf extracts of *Adenantha pavonina*, *BMC Complementary Altern. Med.*, 16 (1), 466.
- [14] Almeida, A.R.R.P., and Monte, M.J.S., 2017, Vapour pressures and phase transition properties of four substituted acetophenones, *J. Chem. Thermodyn.*, 107, 42–50.
- [15] Neese, F., Wennmohs, F., Becker, U., and Riplinger, C., 2020, The ORCA quantum chemistry program package, *J. Chem. Phys.*, 152 (22), 224108.
- [16] Grimme, S., Brandenburg, J.G., Bannwarth, C., and Hansen, A., 2015, Consistent structures and interactions by density functional theory with small atomic orbital basis sets, *J. Chem. Phys.*, 143 (5), 054107.
- [17] Case, D.A., Cheatham III, T.E., Darden, T., Gohlke, H., Luo, R., Merz Jr., K.M., Onufriev, A., Simmerling, C., Wang, B., and Woods, R.J., 2005, The Amber biomolecular simulation programs, *J. Comput. Chem.*, 26 (16), 1668–1688.
- [18] Ibrahim, M.A., Koorbanally, N.A., and Islam, M.S., 2016, Anti-oxidative, α -glucosidase and α -amylase inhibitory activity of *Vitex doniana*: Possible exploitation in the management of type 2 diabetes, *Acta Pol. Pharm.*, 73 (5), 1235–1247.
- [19] Justino, A.B., Guerra Silva, H.C., Franco, R.R., de Oliveira Cavalcante Pimentel, I., Silva, N.F., Saraiva, A.L., and Espindola, F.S., 2022, Flavonoids and proanthocyanidins-rich fractions from *Eugenia dysenterica* fruits and leaves inhibit the formation of advanced glycation end-products and the activities of α -amylase and α -glucosidase, *J. Ethnopharmacol.*, 285, 114902.
- [20] Williams, L.K., Li, C., Withers, S.G., and Brayer, G.D., 2012, Order and disorder: Differential structural impacts of myricetin and ethyl caffeate on human amylase, an antidiabetic target, *J. Med. Chem.*, 55 (22), 10177–10186.
- [21] Sari, B.L., Mun'im, A., Yanuar, A., and Riadhi, R., 2016, Screening of α -glucosidase inhibitors from *Terminalia catappa* L. Fruits using molecular docking method and in vitro test, *Int. J. Pharm. Pharm. Sci.*, 8 (12), 184–189.
- [22] Vaezi, M., Behbehani, G.R., Gheibi, N., and Farasat, A., 2020, Thermodynamic, kinetic and docking studies of some unsaturated fatty acids-quercetin derivatives as inhibitors of mushroom tyrosinase, *AIMS Biophys.*, 7 (4), 393–410.
- [23] Burlingham, B.T., and Widlanski, T.S., 2003, An intuitive look at the relationship of K_i and IC_{50} : A more general use for the Dixon plot, *J. Chem. Educ.*, 80 (2), 214–218.
- [24] Singh, S., Bani Baker, Q., and Singh, D.B., 2022, “Molecular Docking and Molecular Dynamics Simulation” in *Bioinformatics*, Eds. Singh, D.B., and Pathak, R.K., Academic Press, London, UK, 291–304.